Meteorological mechanisms for transporting O_3 over the western North Atlantic Ocean: A case study for August 24-29, 1993

J. L. Moody,[1] J. C. Davenport,[1] J. T. Merrill,[2] S. J. Oltmans,[3] D. D. Parrish,[4] J. S. Holloway,[4] H. Levy II,[5] G. L. Forbes,[6] M. Trainer,[4] and M. Buhr[4]

Abstract. A large-scale view of O_3 transport over the western North Atlantic Ocean (WNAO) in summer illustrates distinct sources of O_3, and separate transport mechanisms are important at different vertical levels in the troposphere. The week-long period presented covers a sequence of O_3 sondes released from Bermuda and encompasses two surface O_3 events in the month-long NARE intensive. O_3 and CO peaked at Chebogue Point on the evening of August 25 and after midnight on the morning of August 28. At Sable Island, peaks occurred during early morning of August 26 and late morning of August 28. These events occurred under W-SW winds associated with advancing low-pressure systems that transported anthropogenic pollutants over the WNAO. The concentrations dropped with the passage of a trough or a cold front. Evidence suggests the surface was occasionally isolated from polluted air during favorable transport with pollutants lifted in warm sector flow riding over a wedge of cool, thermodynamically stable air. In addition to surface O_3, the O_3-sonde profile over Bermuda on the morning of August 27 showed a deep layer of O_3 from 6 to 12 km. Using back trajectories and two tracers (isentropic potential vorticity and water vapor), we illustrate that stratospheric ozone exchanged into the upper troposphere in conjunction with surface cyclogenesis was advected through the middle to upper troposphere over the midlatitudes with the potential to reach lower altitudes through subsidence in regions of anticyclonic motion.

1. Introduction

Ozone is an important atmospheric oxidant and there is concern that its concentration in the troposphere may be increasing [e.g., *Logan*, 1985; *Mohnen et al.*, 1993; *Kley et al.*, 1994]. Both the North Atlantic Regional Experiment (NARE) and the Atmosphere Ocean Chemistry Experiment (AEROCE) have stated objectives to determine the sources of O_3 and/or the processes responsible for its formation and transport over the North Atlantic Ocean [*Fehsenfeld et al.*, this issue(a); *Moody et al.*, 1995; *Oltmans and Levy*, 1993]. Using O_3 and CO data collected at three sites in the Maritime Provinces, *Parrish et al.* [1993] have shown that, in the summer months, high surface O_3 over the WNAO is dominated by anthropogenic pollution. Recent work using back trajectories to interpret 5 years of O_3 and PAN measurements made at Kejimkujik National Park, Nova Scotia, corroborate the importance of transport from east coast source regions in delivering summer O_3 to the surface [*Sirois and Bottenheim*, 1995].

In this paper we present a case study which shows that the type of meteorological conditions which advect significant pulses of polluted air over the NARE study regions are associated with the eastward motion of frontal systems. Warm sector transport (i.e., flow in advance of a surface cold front or trough of low pressure) effectively delivers pollutants from the eastern United States over the midlatitude WNAO. We also illustrate that the upper level dynamics that supports cyclogenesis, the development and deepening of these surface low-pressure systems, is conducive to delivering significant amounts of natural stratospheric O_3 to the upper troposphere. This exchange may occur several days upwind in a tropopause fold or cutoff low. We have observed enhanced O_3 mixing ratios in soundings over Bermuda and have used back trajectories and a dynamic tracer of stratospheric air, isentropic potential vorticity (IPV), to illustrate its origin. *Danielsen and Hipskind* [1980] used this approach to demonstrate that periodic cyclogenesis which intensifies the position of the trough in the mean summer upper air circulation over Alaska and Canada produces a downward and southward transport of stratospheric air into the mean troposphere at polar latitudes. They describe this as a phenomenon similar to that which occurs at lower latitudes in winter and spring. Our analyses, presented here and in the work of *Merrill et al.* [this

[1]University of Virginia, Department of Environmental Sciences, Charlottesville, Virginia.

[2]University of Rhode Island, Graduate School of Oceanography, Narragansett, Rhode Island.

[3]NOAA Climate Monitoring and Diagnostics Laboratory, Boulder, Colorado.

[4]NOAA Aeronomy Laboratory, Boulder, Colorado.

[5]NOAA Geophysical Fluid Dynamics Laboratory, Princeton, New Jersey.

[6]Atmospheric Environment Service, Downsview, Ontario, Canada.

issue], indicate that a natural source of O_3 to the midlatitude midtroposphere is significant even in the summer. In fact, observations made in August 1989 show evidence of similar meteorological conditions which appear to have influenced O_3 concentrations observed on one of the GTE/CITE flights over the WNAO [Shipham et al., 1993; Anderson et al., 1993].

In this paper we seek to illustrate the dynamic connection between the meteorological conditions which deliver high O_3 concentrations (~ 100 ppbv) from anthropogenic sources to the lower midlatitude WNAO troposphere and the meteorological conditions which result in stratospheric/tropospheric exchange of O_3 into the upper troposphere. These exchange conditions and subsequent transport are proposed as a plausible mechanism to explain the observations of enhanced O_3 concentrations (~ 100 ppbv) in the upper troposphere over Bermuda.

2. Data and Methods

2.1. Chemical Data and Sampling Methods

Chemical data from two different sources are reported in this paper. Surface chemical measurements made as part of the NARE field intensive included continuous O_3 and CO observations on Sable Island and at Chebogue Point, Nova Scotia [Fehsenfeld et al., this issue(b)]. Data for these locations have been plotted as 10-min averages, based on all 1-min averages recorded in each 10-minute period. Data for periods with 10-minute standard deviations greater than 2 ppbv O_3 or 20 ppbv CO were removed from the data set. At each site, concentrations were measured 10 m above the ground using a TECO model 49 instrument based on ultraviolet absorption for O_3 and a TECO model 48 based on nondispersive infrared absorption for CO [see Parrish et al., 1994]. In collaboration with NARE, vertical profiles of O_3, temperature, and frost point were measured on balloonborne Electro-Chemical Cell ozonesondes released from Bermuda [Oltmans et al., this issue].

2.2. Meteorological Data and Methods

Back trajectories have been calculated using two different methods. For trajectories in the lower troposphere over the Gulf of Maine, the NOAA ARL Hy-Split model was used [Draxler, 1992]. These model runs were based on the regional scale wind and temperature fields of the National Meteorological Center nested-grid model (NMC-NGM) [Hoke et al., 1989]. Applying Hy-Split, we have calculated 72-hour, three-dimensional back trajectories that used the NGM's dynamically consistent vertical velocities calculated on 10 terrain-following σ levels between the surface and ~400 hPa. Two plot frames are used to display each trajectory, the latitude/longitude map projection shows the trace of geographical history for each hypothetical air mass, while the vertical cross section shows pressure as a function of time back along the trajectory. This view illustrates regions of relative upward and downward motion for each trajectory. To illustrate the evolution of synoptic conditions, we have also plotted maps of surface pressure and 1000-hPa temperature fields and the 250-hPa geopotential height and relative vorticity (simply a measure of rotation in the wind velocity field) based on the NGM initialization.

The high-resolution meteorological fields of the NMC-NGM cover a relatively limited subregion of the northern hemisphere, primarily the continental United States, and a small surrounding boundary. Therefore to calculate back trajectories from Bermuda, we had to rely on the NMC global analysis. The University of Rhode Island's (URI) isentropic back-trajectory model [Merrill, 1994; Merrill et al., 1986] was run for several potential temperature (θ) levels at 5 K intervals, from 320 K to 350 K. Isentropic trajectory models do not take account of the grid-scale vertical velocity in the meteorological fields; the vertical motion is approximated by adiabatic motion along sloping surfaces of potential temperature. Trajectory plots in this paper illustrate the θ level as a bold label on the latitude/ longitude map projection of the transport path. A second panel displays a pressure/longitude cross section which corresponds to relative changes in the geopotential height of the theta surface.

In addition to trajectories, we have calculated isentropic potential vorticity (IPV) [see Merrill et al., this issue], which is simply the potential vorticity on an isentropic (constant θ) surface. The following equation illustrates that potential vorticity is the product of two terms. The first term is the vertical component of the absolute vorticity, the second term is a measure of the atmospheric static stability.

$$IPV = PV_\Theta = \left[f + \left(\frac{\partial u}{\partial y}\right)_\Theta - \left(\frac{\partial v}{\partial x}\right)_\Theta \right] \cdot \left[-g\frac{\partial \Theta}{\partial P} \right]$$

Air in the stratosphere has high static stability and, as a result, high IPV. Values greater than 1.5 IPV units (1.5 X 10^{-6} m^2 s^{-1} K kg^{-1}) are typically found only in the stratosphere; thus IPV can be used to define the tropopause level. Because it is quasi-conservative (under adiabatic conditions), it can also be used to trace ozone-rich air which has moved from the stratosphere to the troposphere [Danielsen and Hipskind, 1980]. Danielsen et al. [1987] proposed that atmospheric chemists should be able to use positive correlations of ozone and potential vorticity and negative correlations of water vapor mixing ratio and potential vorticity to identify air of stratospheric origin. He further suggested that these correlations might be used to derive quantitative estimates of stratospheric-tropospheric exchange.

Through the use of potential vorticity calculated on isentropic surfaces (IPV), in conjunction with isentropic trajectories, we have identified air parcels in which the ozone is likely to have originated in the stratosphere. IPV fields in this paper have been calculated using an objective analysis based on rawinsonde measurements of wind and temperature from two isentropic surfaces 10 K apart, centered on the specified potential temperature level. The North American rawinsonde data were carefully screened for the dates analyzed in this paper (August 21-29, 1993), with either the bad datum or the entire sounding removed when obvious errors were found. The screened data were objectively analyzed using a modified Barnes analysis [Hibbard and Wiley, 1985] to produce gridded isentropic maps for θ levels 315 through 345. Absolute vorticity was calculated for each θ surface. We calculated the inverse static stability (a measure of how close together the pressure surfaces were for a

given change in potential temperature) using finite differences in the pressure field for a layer between ± 5 K on either side of the designated θ surface. This method is not identical to the one presented by *Merrill et al.* [this issue], in this case the data were screened by visual inspection of soundings, and calculations were performed using the McIDAS system. The advantages of the IPV model described by *Merrill et al.* [this issue] are the consistent data-checking criteria and a more sophisticated analytical method for calculating the partial differentials. Nonetheless, we have intercompared IPV fields calculated by using these different schemes for a few days, and we are confident the features reported in this paper are indeed significant and robust.

The location of calculated trajectories and IPV analyses have been overlaid onto color-enhanced satellite images which show the remotely sensed water vapor channel from GOES-7. This is a derived product that is temperature dependent and weighted toward the 400-hPa level, therefore it is essentially a midtroposphere relative humidity. These data have been displayed as an effective corroboration of the presence of dry air associated with intrusions from the stratosphere into the troposphere.

3. Results

In the following sections we describe a subset of the chemical and meteorological observations made during the NARE August 1993 intensive. First, in section 3.1 we present NARE surface chemical data and describe modeled air parcel transport. In section 3.2 we describe the synoptic scale meteorological conditions at the surface and aloft which led to the observed transport and chemical signals. Then we present ozonesonde profiles (section 3.3) for Bermuda which cover the same time period and we link these to meteorological conditions in the middle to upper troposphere with calculations of upper level trajectories and associated tracer fields of IPV and water vapor (section 3.4).

3.1. Surface Ozone

Figure 1 shows the time series of O₃ and CO for the last week of August 1993 at Chebogue Point and Sable Island. Instruments at the NARE surface site at Chebogue detected a peak in concentrations of 78 ppbv O₃ and 245 ppbv CO at 0000 UTC on August 26 (2000 AST on August 25). Back trajectories indicate westerly winds in the flow associated with a trough of low pressure moving offshore with advancing warm air (Figure 2a). This warm frontal flow was followed by a relative shift to northwesterly winds associated with the eastward moving trough and the ridge of high pressure moving into the northeast United States (Figure 2b); however, there was no cold front associated with this trough. (This is apparent in the isotherms plotted on the surface maps shown in the next section (Figures 6a and 6d)). The warm frontal flow that reached Sable Island a few hours later was enriched in CO and had slightly enhanced O₃ concentrations. The peak in O₃ occurred at 0640 UTC with 47 ppbv O₃ and 154 ppbv CO (Figure 3a). The CO continued to climb and peaked at 179 ppbv at 1340 UTC with O₃ of 41 ppbv. These concentrations are much lower than those observed at Chebogue Point.

As the wind shifted to NW with the passage of the trough of low pressure, the concentrations at Chebogue fell to
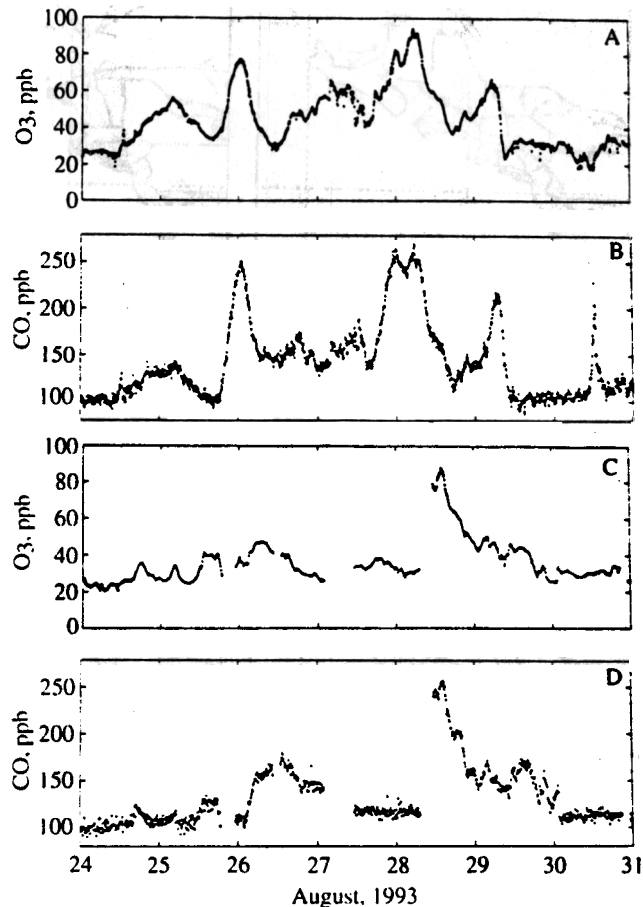
Figure 1. Time series of 10-min average O₃ (top boxes) and CO (bottom boxes) concentrations measured at (a) Chebogue Point and (b) Sable Island during last week of August (24-31) 1993.

28 ppbv and 147 ppbv O₃ and CO, respectively, by 1000 UTC August 26 (0600 AST) (Figure 2c). This drop in concentration was likely aided by the extremely stable conditions present at Chebogue on the morning of August 26 as evidenced by a significant low-level inversion over the site (see *Merrill and Moody*, Figure 6b, [this issue]) which would prohibit mixing of any elevated pollution into the surface layer. At Sable Island the wind shift indicated by back trajectories occurred around 1200 UTC on August 26, and the chemical concentrations began to fall (Figure 3b).

Concentrations of Chebogue Point O₃ increased throughout the afternoon on August 26 under NW flow around high pressure and peaked at 65 ppbv around 0400 UTC on August 27 (midnight on August 26, Figure 2d). Trajectories show the wind backed with time from northwesterly to southwesterly, indicative of warm air advection in this layer; and, by 2000 UTC (1600 AST) on the afternoon of August 27, a new stronger frontal system was pushing a very warm air mass out over the ocean (Figure 2e). At Chebogue Point, concentrations of 61 ppbv of O₃ and 195 ppbv of CO were observed at 2000 UTC, increasing very rapidly to 88 ppbv O₃ and 253 ppbv CO by midnight (0400 UTC on August 28). Concentrations peaked between 0100 and 0200 (0540 UTC) on August 28, with the back trajectories
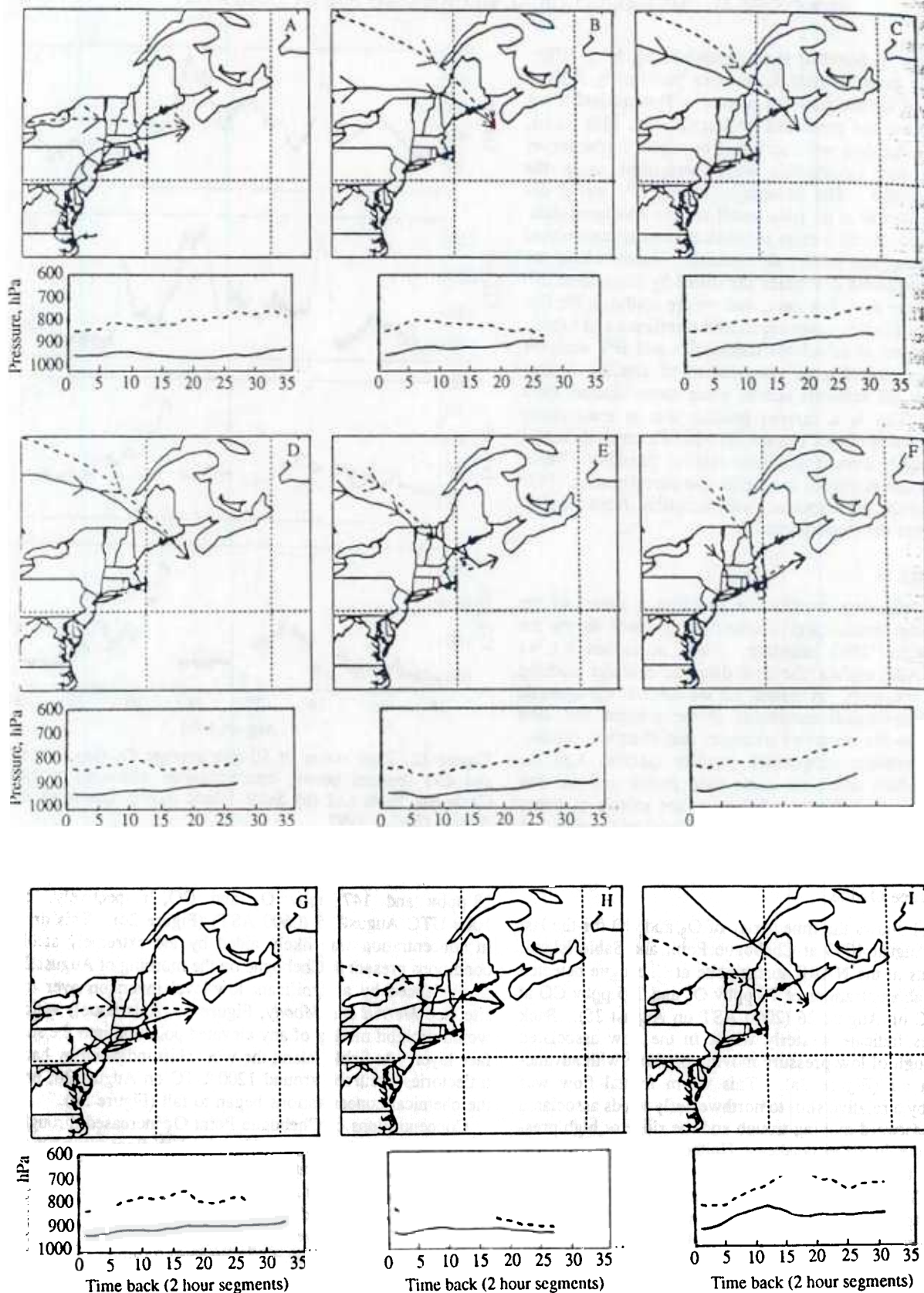
Figure 2. The 500- (solid line) and 1500-meter (dashed line) back trajectories depicting transport to Chebogue Point at specific times calculated with the Hy-split model and plotted with endpoints marked with arrowheads indicating the direction of motion at 12-hour intervals; sizes of arrowheads are proportional to wind velocity over the preceding 2 hours. Times are (a) August 25, 2000 UTC; August 26, (b) 0400 UTC and (c) 1200 UTC; August 27, (d) 0400 UTC and (e) 2000 UTC; August 28, (f) 0400 UTC and (g) 1600 UTC; and August 29 at (h) 0400 UTC and (i) 1200 UTC.
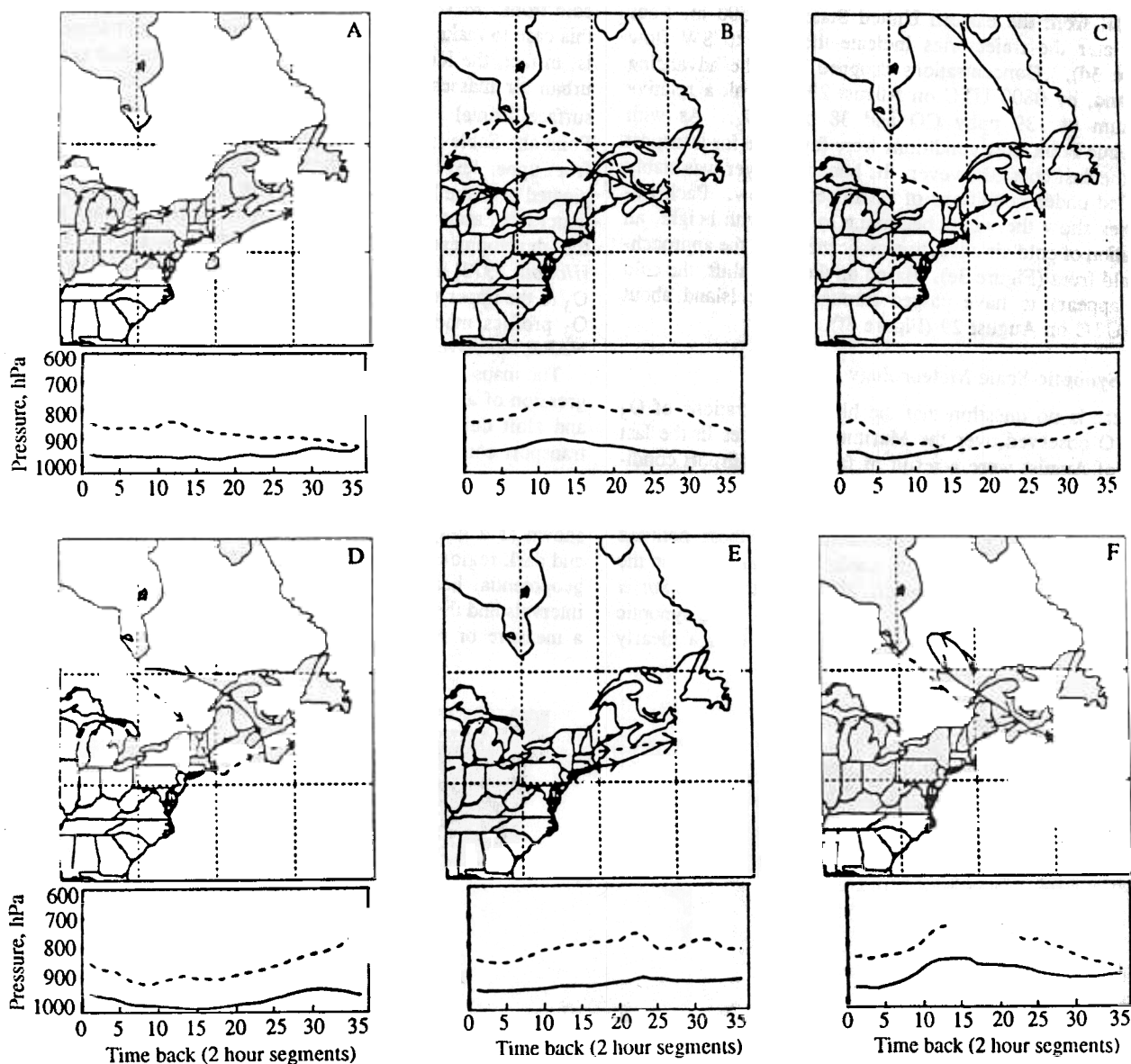
Figure 3. The 500- (solid line) and 1500-meter (dashed line) back trajectories depicting transport to Sable Island at specific times calculated with the Hy-split model and plotted with endpoints marked with arrowheads indicating the direction of motion at 12-hour intervals; sizes of arrowheads are proportional to wind velocity over the preceding two hours. Times are August 26, (a) 0400 UTC and (b) 1200 UTC; August 27, (c) 2000 UTC; August 28, (d) 1200 UTC and (e) 1600 UTC; and August 29, (f) 2000 UTC.

indicating very rapid transport from the east coast, with an air mass arriving from a region that 12 hours earlier had been under relatively stagnant conditions in the vicinity of major urban source regions of New York and New Jersey (Figure 2f).

Concentrations fell throughout the day on August 28, reaching a minimum at 1800 UTC (1400 AST) of 37 ppbv O₃ and 114 ppbv CO. Regional-scale transport conditions were still favorable (Figure 2g); however, meteorological data from the site indicated an elevated inversion that contributed to isolating the much cooler surface layer from warmed daytime layers of pollution aloft [see *Angevine et al.*, this issue]. On the regional scale, flow conditions indicate favorable transport in the warm sector of a well-

developed frontal system on the afternoon of August 28 [see *Merrill and Moody*, Figure 9, this issue]. A cold front was advancing and concentrations rose to a peak of 67 ppbv O₃ and 205 ppbv CO at 0575 UTC (0145 am) on August 29. As the cold front went through, winds shifted to northwesterly (Figure 2h), and concentrations plummeted to 30 ppbv O₃ and 100 ppbv of CO by morning (1200 UTC) (Figure 2i).

At Sable Island this event was observed as a maximum in CO (254 ppbv) and O₃ (88 ppbv) at 1400 UTC (1000) on August 28; these concentrations are comparable to those observed at Chebogue Point. Trajectories at this time indicate significant wind shear, winds backed with height, indicative of warm air advection (Figure 3c). Flow at the

surface (500 m) was from the north, but there was favorable transport from the eastern United States at 1500 m. Four hours later the trajectories indicate the shift to SW flow (Figure 3d). Concentrations dropped with the advancing front and, by 0800 UTC on August 29, they hit a relative minimum of 139 ppbv CO and 38 ppbv O_3. As with Chebogue Point flow conditions were favorable for transport from the east coast; however, the boundary layer was stably stratified under conditions of warm sector flow. Back trajectories show the winds beginning to veer with height, an indication of cold air advection associated with the approaching cold front (Figure 3e). Based on the wind shift, the cold front appears to have passed through Sable Island about 2000 UTC on August 29 (Figure 3f).

3.2. Synoptic-Scale Meteorology

There is no question that the high concentrations of O_3 and CO observed over the Maritimes Provinces in the last week of August were a result of favorable transport conditions which delivered pulses of anthropogenically polluted air to the lower troposphere. Several other papers in this issue better illustrate the elevated nature of these polluted parcels, lifted over the cool, stable, stratified air near the ocean surface [*Kleinman et al.*, this issue(a); *Kleinman et al.*, this issue(b); *Angevine et al.*, this issue]. The synoptic system on August 28 was well developed with a clearly

defined warm sector between a warm front and an advancing cold front. *Merrill and Moody* [this issue] have generalized this case to make the observation that warm sector transport is, in fact, the ideal synoptic condition to deliver east coast urban air masses to the midlatitude WNAO. Both of the surface frontal systems which delivered O_3 to Chebogue Point and Sable Island during this week derived their energy from upper level waves and associated vorticity which originated over the Pacific Northwest. We hypothesize that the upper level atmospheric dynamics which were necessary for the development of the frontal systems at the surface [*Holton*, 1972] also delivered significant amounts of natural O_3 to the upper troposphere out over the NAO. A series of O_3 profiles made over Bermuda during the period of the NARE intensive support this hypothesis.

The maps shown in Figures 4, 5, and 6 illustrate the progression of and relationship between weather at the surface and aloft during the week leading up to the ideal NARE transport conditions observed on August 28. The top row is surface data, with sea-level pressure presented with contour lines at 4-hPa intervals and the 1000-hPa temperatures shown as a gray-scale field where light regions are warm and dark regions are cool. The bottom row shows 250-hPa geopotential heights (~ 340 K) as contour lines at 40-m intervals and the vertical component of the relative vorticity, a measure of rotation, as a gray-scale field (dark regions
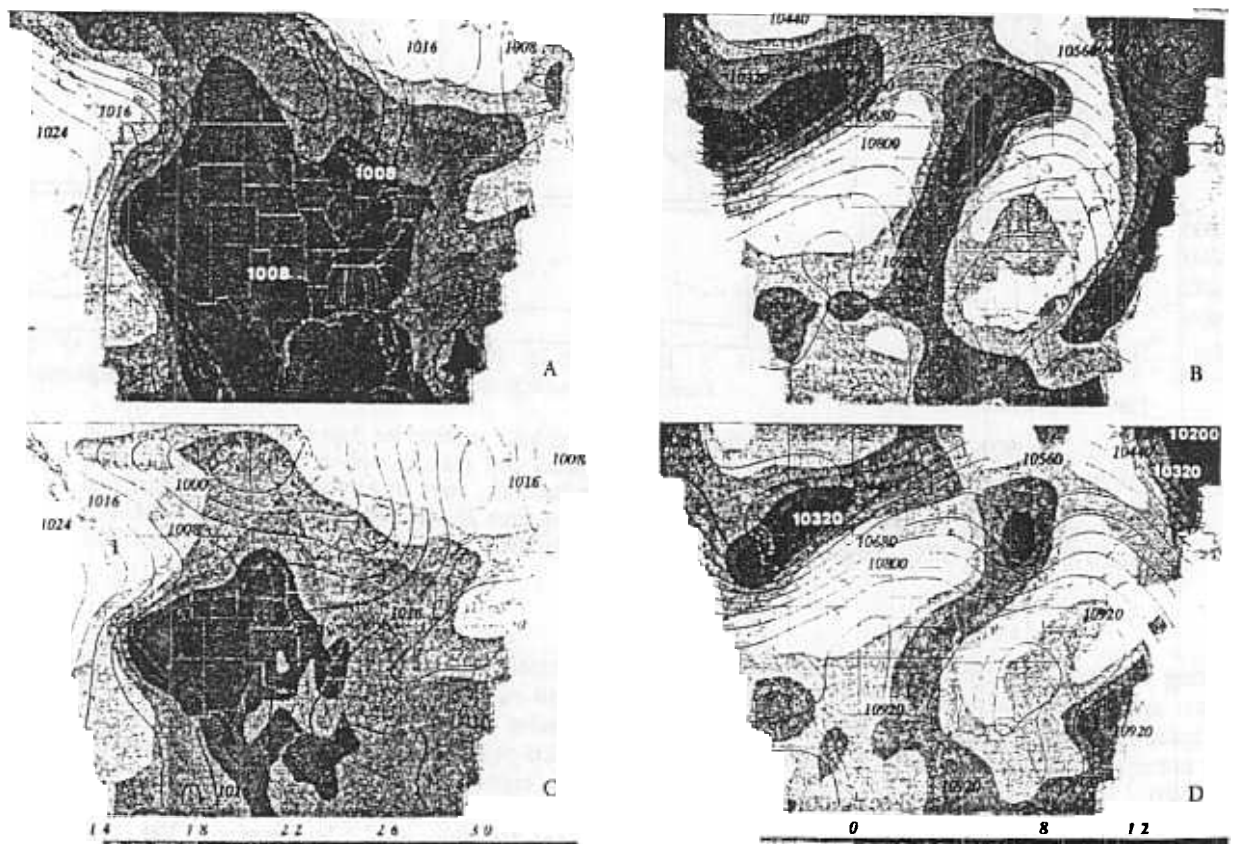
Figure 4. Surface weather maps (pressure contours in black; 1000-hPa temperatures in underlying shades of grey) for (a) 0000 UTC and (c) 1200 UTC, August 24. Upper air maps show 250-hPa traveling waves (geopotential height contours in black, relative vorticity in underlying shades of grey; positive cyclonic vorticity in dark colors) for (b) 0000 UTC and (d) 1200 UTC, August 24.
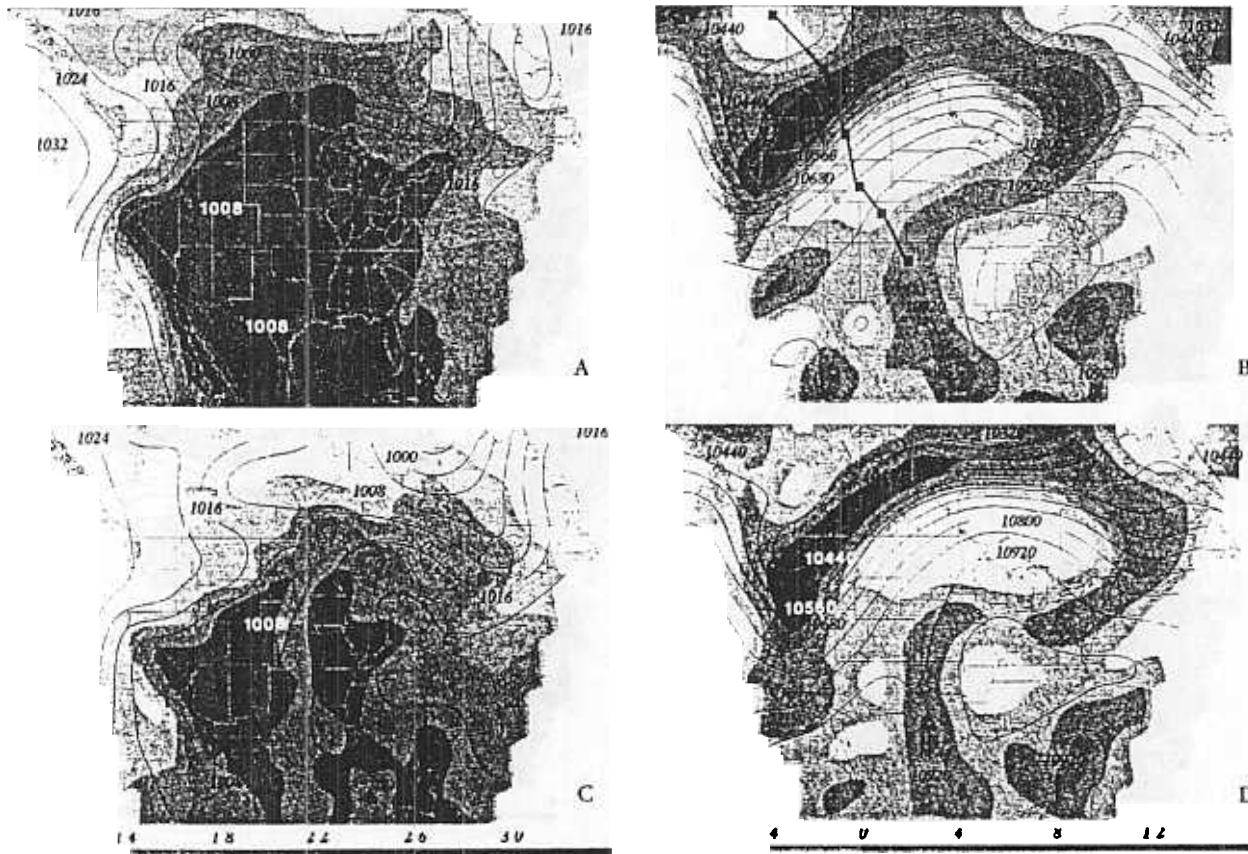
Figure 5. Surface weather maps (pressure contours in black; 1000-hPa temperatures in underlying shades of grey) for (a) 0000 UTC and (c) 1200 UTC, August 25. Upper air maps show 250-hPa traveling waves (geopotential height contours in black; relative vorticity in underlying shades of grey; positive cyclonic vorticity in dark colors) for (b) 0000 UTC and (d) 1200 UTC, August 25. Bold line on Figure 5b shows location of cross section in Figure 8; each box shows location of a rawinsonde site.

indicate large values of positive relative vorticity which represents cyclonic rotation).

In the first column (Figure 4a), 0000 UTC August 24 (Julian day 236), there was a surface low near the United States-Canadian border over the Great Plains and very warm air over the western United States. At 250 hPa a short wave was moving across the central United States (Figure 4b). A lobe of positive relative vorticity (as well as IPV, not shown) extended southward into Texas. Twelve hours later the surface low had deepened (Figure 4c). The lower temperatures in this figure are mostly the diurnal variation evident in going from 0000 UTC to 1200 UTC. The short wave at 250 hPa lost amplitude blocked by high pressure over the SE United States that extended up to 250 mbar (Figure 4d). A region of high relative vorticity was centered over upper Michigan at this time.

By 0000 UTC on August 25, at the surface there was a significant trough and a weak warm front, which can be seen in the isotherms as warm air pushing over the NE United States into Canada (Figure 5a). This trough deepened in association with the short wave at 250 mbar and the positive vorticity advection associated with its movement. A new upper level wave associated with a strong jet stream was moving into the Pacific Northwest (Figure 5b) and developed a cutoff low. The energy associated with this system

would go on to develop the surface system which influenced the Maritime Provinces on August 28 and 29. This wave generated a large region of high relative vorticity and IPV over Washington, Oregon, Idaho, and Montana. By 1200 UTC on August 25, the warm air at the surface was over Vermont, New Hampshire, and Maine and moving out over the Gulf of Maine as a weakened trough pushed offshore (Figure 5c). This trough was analyzed on surface maps as a southward extension of the warm front through Quebec, connected with the low over Hudson Bay. The long wave at 250 mbar over the northwest deepened and moved eastward (Figure 5d).

Figure 6 skips ahead in time and shows the meteorological conditions associated with the system that delivered high surface ozone to the maritimes on August 28 and 29. The surface map at 0000 UTC on August 28 shows a low pressure system over Ontario and Quebec (Figure 6a). There was warm air pushing out over the Gulf of Maine and a cold front through Michigan and Ontario seen as the leading edge of cool air in the isotherms. There was still considerable energy at 250 mb, with the short wave north of Lake Superior associated with a region of intense cyclonic vorticity (Figure 6b). Twelve hours later, at 1200 UTC, the low pressure at the surface had deepened; there was a well-developed warm sector between a warm front (running
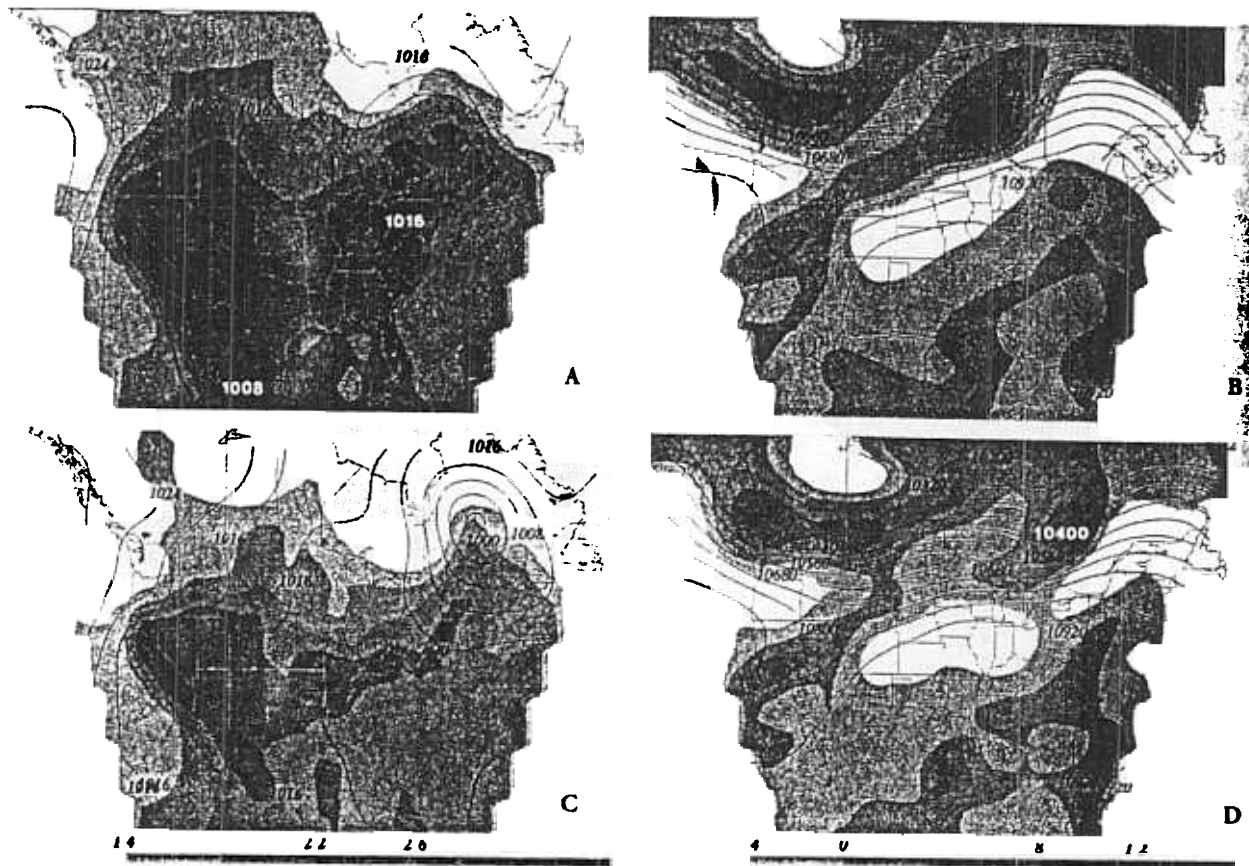
Figure 6. Surface weather maps (pressure contours in black; 1000-hPa temperatures in underlying shades of grey) for (a) 0000 UTC and (c) 1200 UTC, August 28. Upper air maps show 250-hPa traveling waves (geopotential height contours in black; relative vorticity in underlying shades of grey; positive cyclonic vorticity in dark colors) for (b) 0000 UTC and (d) 1200 UTC, August 28.

through Nova Scotia) and the cold front through New York clearly visible in the isotherms (Figure 6c). The short wave was over the Ontario/Quebec border, and the ridge of high heights that had dominated at 250 hPa earlier in the week had given way to nearly zonal flow.

3.3. Ozonesonde Profiles

An "intensive" series of O_3 soundings was made over Bermuda near the end of August, with launches on August 20, 24, 25, 27, 28, 29, and 30. This series effectively began on August 20, with concentrations of the order of 25 ppbv in the lowest 2 km, climbing to an average of 60 ppbv in the middle troposphere, from 4 to 8 km (Figure 7a). The O_3 and frost point temperature suggest this layer of dry air was relatively low in O_3. Above 8 km concentrations increased to the order of 75 ppbv (at the 340 K θ level) and remained in this range until they increased dramatically in the lower stratosphere, above 13-14 km. By August 24 (Figure 7b) the concentrations between 2 and 8 km were significantly higher, and a layer of high O_3 above 100 ppbv was observed between 11 and 14 km (θ of 340-345 K). The next day (August 25) the concentrations were slightly lower below 8 km and concentrations in the upper troposphere increased dramatically above 12 km (θ=345 K) (Figure 7c). By August 27 there was a deep column of enhanced O_3

with concentrations ranging from 80 to 130 ppbv between 6 and 12 km (325 to 345 K) over Bermuda (Figure 7d). One day later, however, the midtroposphere from 5 to 8 km saw significantly lower O_3 mixing ratios with concentrations at the 335 K θ level dropping from 110 ppbv to 59 ppbv of O_3 (Figure 7e). The mixing ratios in the upper troposphere dropped significantly (e.g., from 126 ppbv to 47 ppbv at 345 K), and there were two relative maxima in O_3 defining layers between 320 and 325 K and 335 and 340 K. On August 29 the O_3 continued to exhibit two relative maxima with layers present in the same potential temperature ranges. However, in the 10- to 13-km region, ozone mixing ratios had decreased further with only 28 ppbv of O_3 at 345 K. Analysis of satellite water vapor images clearly indicates that the upper level portion of this profile was influenced by the cirrus shield of Hurricane Emily which was just south of Bermuda at this time.

3.4. Isentropic Potential Vorticity and Water Vapor

In this section synoptic IPV fields are presented superimposed on color-enhanced satellite images of the water vapor channel. The isentropic potential vorticity is a measure of both absolute vorticity and static stability. The absolute vorticity is a function of latitude and the relative vorticity, which is a function of the wind field. Relative vorticity
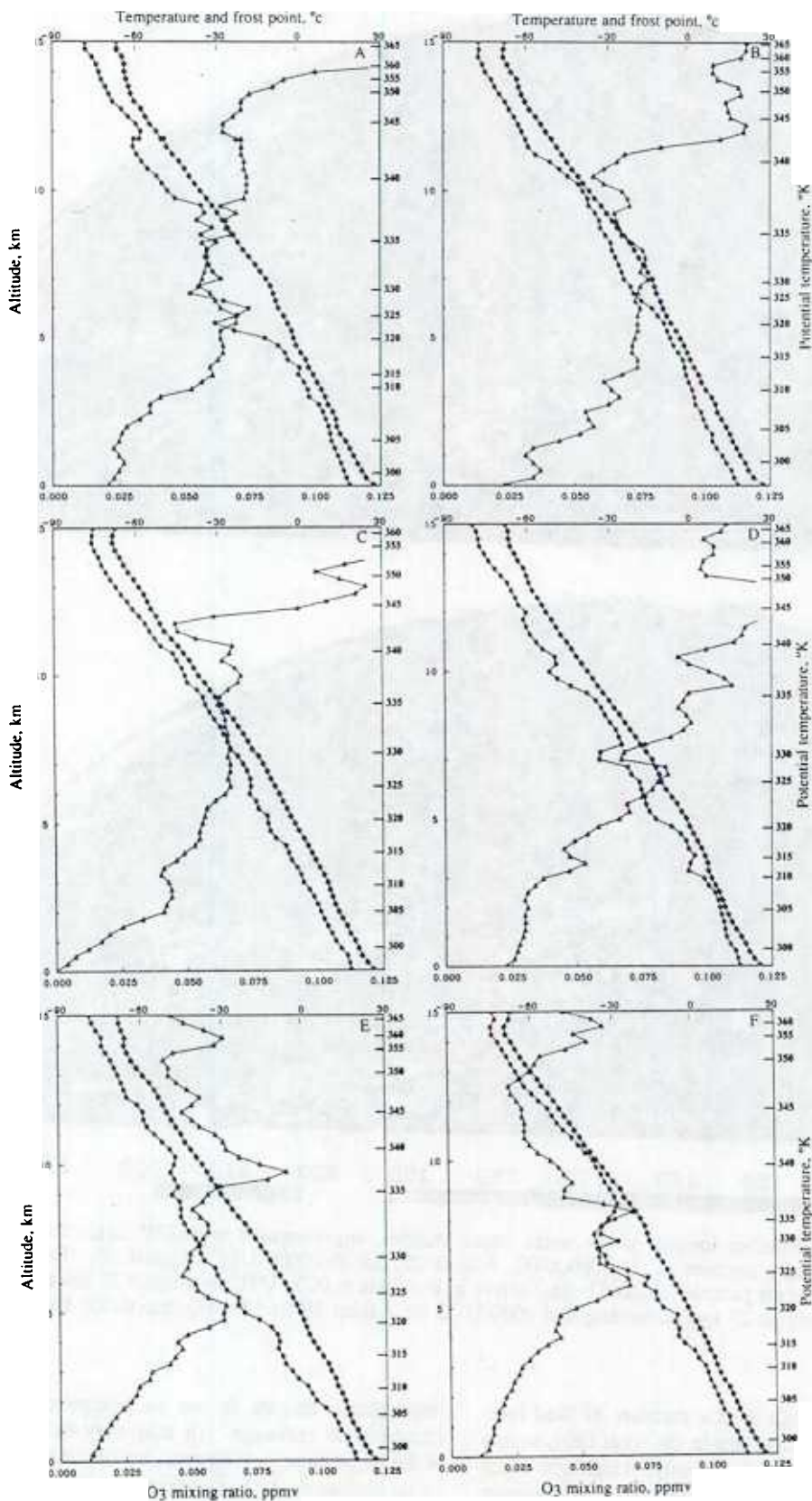
Figure 7. Bermuda ozonesonde profiles of O_3 (triangles) showing air temperature (diamonds) and frost point (circles) as a function of height on (a) August 20, (b) August 24, (c) August 25, (d) August 27, (e) August 28, and (f) August 29. Potential temperature is plotted as a function of height on the right of the figure, with surfaces marked at 5-K intervals from 300 K to 365 K.

130   140   150   160   170   180   190   200   210   220   230
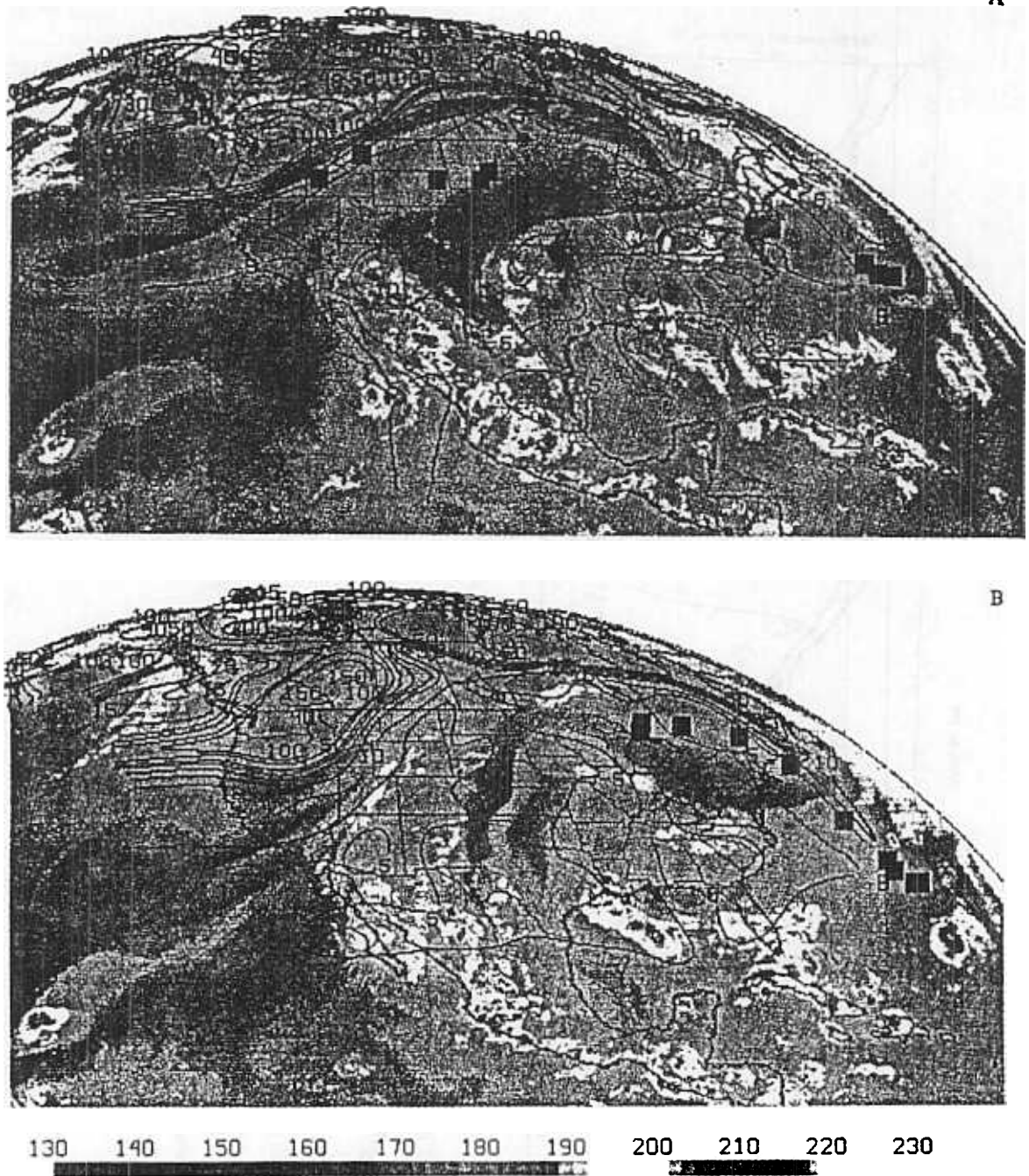
Plate 1. Satellite images of the water vapor channel, superimposed with IPV fields for 330 K potential temperature surfaces at (a) 0000 UTC, August 25, and (b) 0000 UTC, August 26. The 330 K trajectory-modeled air parcels (colored boxes) arrive in Bermuda at 0000 UTC on August 27 (blue boxes), 1200 UTC on August 27 (green boxes), and 0000 UTC on August 28 (red boxes) (see Color Plate 2).

(shown in Figures 4 through 6) is a measure of fluid rotation, which may indicate curvature in the wind field, such a flow through a trough, or shear vorticity, which can occur even in zonal flow if the wind speed changes perpendicular to the axis of the flow. This is typical of flow around the jet stream. The stratosphere, where temperature is constant or increases with height, has very high static stability, so regions of high relative vorticity near the tropopause, will be regions of high IPV. The presence of high IPV values at

tropospheric heights is not an unequivocal indication of stratospheric exchange. (It may only indicate deformation of the tropopause.) However, by plotting the value of IPV on an isentropic surface, regions of high values of IPV at relatively low tropospheric heights will represent regions where stratospheric exchange may occur.

In order for exchange to occur, nonadiabatic terms must be considered (i.e., diabatic or turbulent mixing [*Lamarque and Hess*, 1994; *Shapiro*, 1980]). In Plates 1 and 2 we
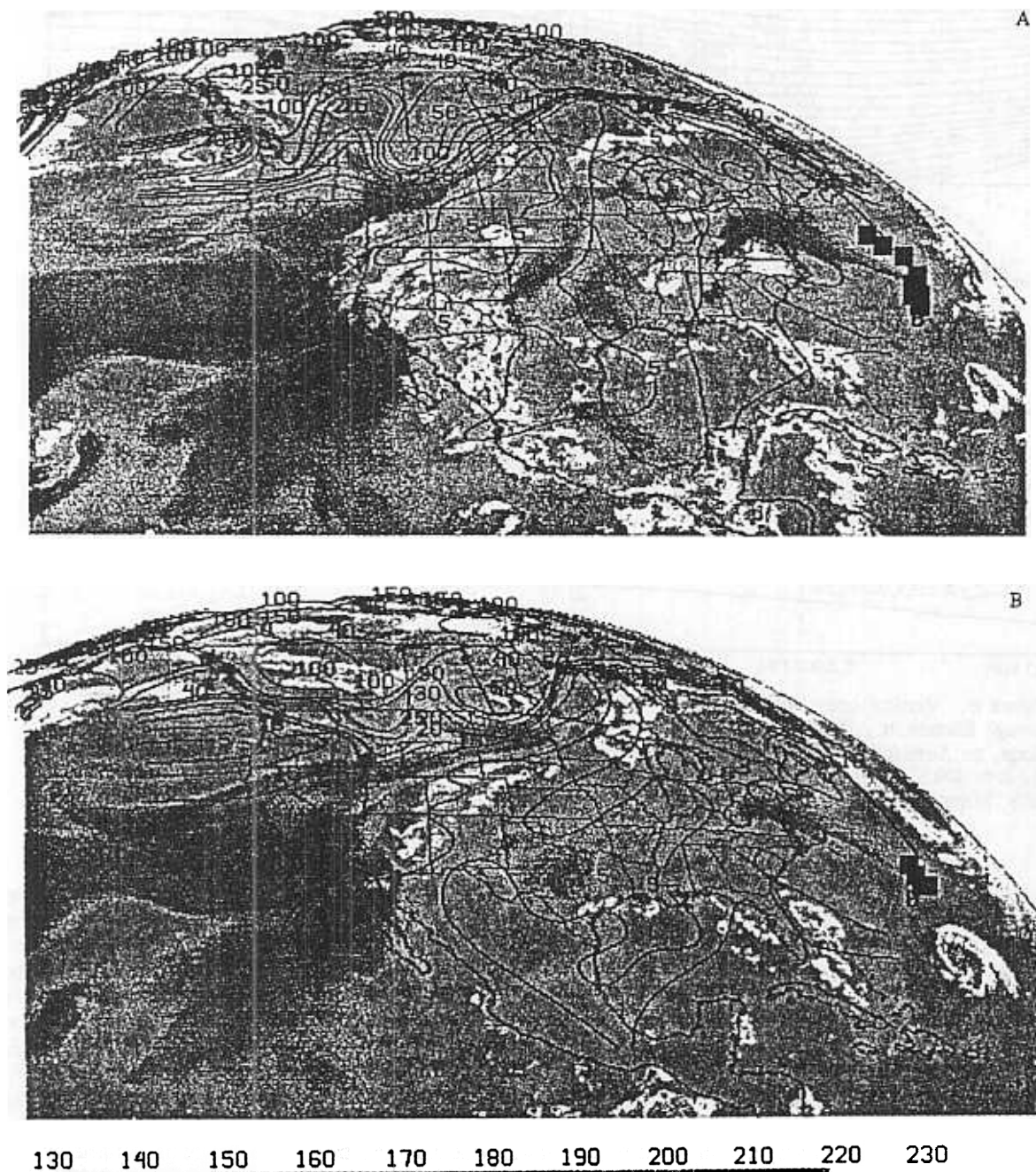
Plate 2. Satellite images of the water vapor channel, superimposed with IPV fields for 330 K potential temperature surfaces at (a) 0000 UTC, August 27, and (b) 1200 UTC, August 27. The 330 K trajectory-modeled air parcels (colored boxes) arrive in Bermuda at 0000 UTC on August 27 (blue boxes), 1200 UTC on August 27 (green boxes), and 0000 UTC on August 28 (red boxes) (see Color Plate 1).

show that exchange across the tropopause along the jet stream 2 days upwind of Bermuda is likely to make a significant contribution to the enhanced O$_3$ observed in the upper troposphere over Bermuda on the August 27. There is good evidence of tropopause folding when we look at vertical cross sections through the trough and when we look at the water vapor signal. Plotting the remotely sensed water vapor field, the dark blue regions are characteristic of very dry air and show good correspondence to the leading edge of high IPV. *Appenzeller and Davies* [1992] have

shown this to be an excellent indicator of stratospheric intrusions. Together, the panels of Plates 1 and 2 show motion on the 330 K isentropic surface. In addition to water vapor and 330 K IPV fields, each image shows a trajectory snapshot: the current position of air parcels on the 330 K surface that will eventually arrive at four endpoints surrounding Bermuda. The back trajectories were started at three different times, 0000 and 1200 UTC on August 27 and 0000 UTC on August 28 (at the designated 330 K θ level). The different times are indicated by the large colored boxes,
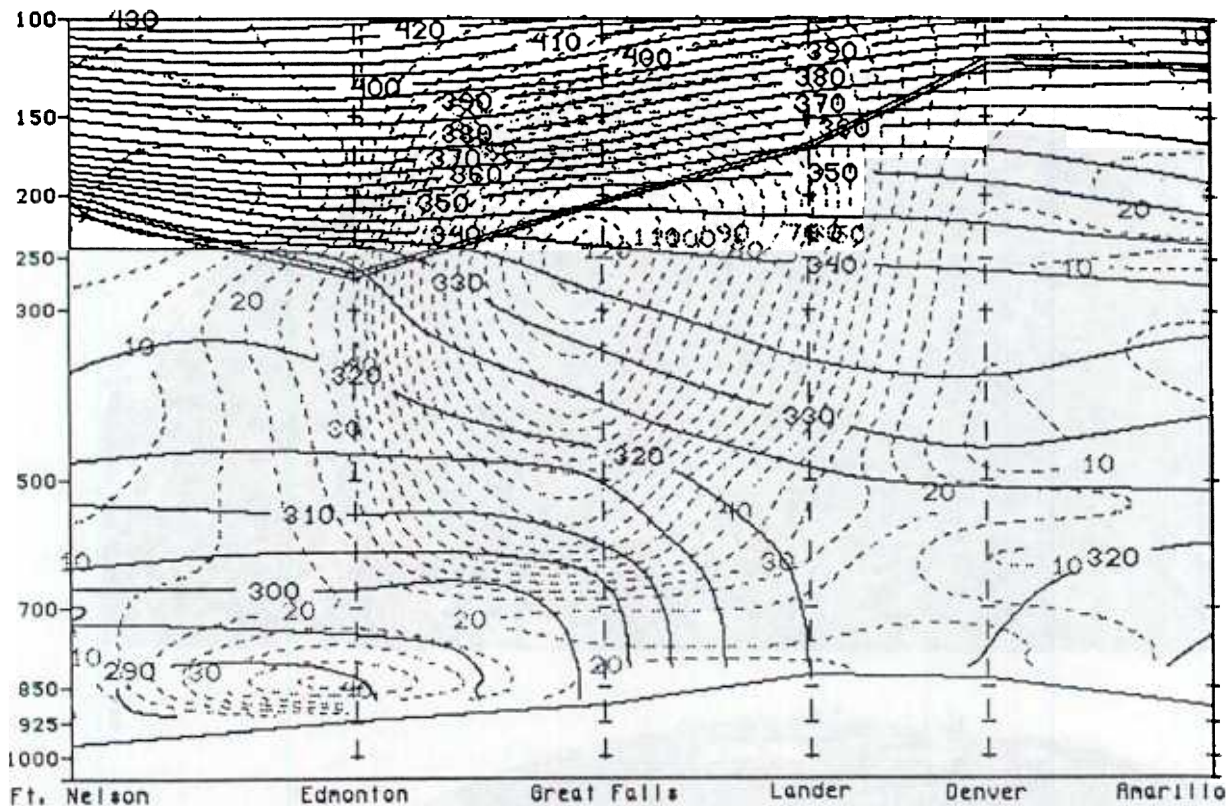
Figure 8. Vertical cross section through the upper level trough from Fort Nelson, British Columbia, through Edmonton, Alberta; Great Falls, Montana; Lander, Wyoming; and Denver, Colorado; to Amarillo, Texas, on August 25 (see Figure 5b). Potential temperature is plotted versus pressure (solid lines) from 290 K to 400 K. Isotachs of wind velocity (dashed lines) have a maximum jet speed of 120 knts over Great Falls, Montana, at 250 mb. Double line is height of standard tropopause from rawinsonde observations.

blue boxes represent the air which arrives in Bermuda on August 27 at 0000 UTC, green boxes indicate the air that arrives at 1200 UTC on August 27, and red boxes show the location of air that arrives in Bermuda at 0000 UTC on August 28.

Plate 1a shows the water vapor distribution for 0000 UTC, August 25. At this time there was a region of very high IPV over the Pacific Northwest with maximum values greater than 15 IPV (the units plotted in Plates 1 and 2 are IPV x 10^{-1}). The bright blue region just south of this maximum indicates an intrusion of very dry air to the south of the wind maximum associated with the upper air pattern. In fact, the long ribbon of blue which runs from the California coast to Hudson Bay corresponds very well to the edge of the gradient in IPV and effectively outlines the region of the jet stream. This remotely sensed water vapor signal is weighted toward 400 mb and shows that very dry air has penetrated to midtropospheric heights. The blue boxes in this plate (and Plate 2) show the location of isentropically modeled air parcels which arrive at four points surrounding Bermuda at a potential temperature level of 330 K at 0000 UTC on August 27 (2 days later). These represent air parcels under the relatively stagnant Bermuda high. By contrast, air parcels that arrive at 1200 UTC on August 27 and 0000 UTC on August 28 were over the western United States. The parcels that arrive at 1200 UTC in particular appear to move along the edge of the dry air associated with high IPV.

There is additional evidence of tropopause folding occurring along this feature, with stratospheric air moving from the poleward side of the jet beneath and to the equatorward side of the jet, producing the observed dry zone imprint in the water vapor signal. Figure 8 shows a cross section from Canada to Texas, which illustrates the classic break in the tropopause, with the stratosphere much lower on the poleward side of the jet. The stratosphere is easily identified as the region of potential temperature rapidly increasing with height (high static stability). The rawinsonde-analyzed tropopause height is defined by the double line which varies between 250 hPa and 130 hPa. The IPV field for the 330 K potential temperature surface shown in Plate 1a indicates a strong gradient of IPV between Edmonton and Great Falls, Montana, consistent with the location of the jet in this cross section. We can see that the 330 K surface slopes from the lower stratosphere on the poleward side of the jet well into the troposphere on the equatorward side of the jet. The trajectories suggest very rapid motion from this region, which represents a source of stratospheric ozone, to the vicinity of eastern Ontario in 24 hours. Although we have only illustrated transport at the 330 K level, which is the base of the layer of elevated O₃ over Bermuda on August 27, similar transport was observed at higher theta levels.

By 0000 UTC on August 26 (Plate 1b), the air parcels that arrive in Bermuda on August 27 and 28 moved to a location over Quebec or even the Gulf of Maine. They are

still on the edge of the gradient in IPV which has also advanced eastward. Within another 12 hours (Plate 2a, 0000 UTC August 26), we can see a streak of dry air evident as a thin band of blue in the water vapor field. This is the southern edge of the dry air which is advancing toward Bermuda. Although we do not trace high IPV all the way out to Bermuda, we are hampered by a lack of meteorological data over this region which limits our ability to calculate IPV. The trajectories suggest the motion of the air parcels has nearly stalled as they subside anticyclonically into the relative high pressure. Finally, in Plate 2b, the day of the sounding, we see the 1200 UTC air parcels (the green trajectory endpoints) have already arrived in Bermuda with an enhancement of O₃ evident in the sounding. However, the driest air (and perhaps the highest ozone) stays to the north of the site. In this image we can clearly see the approach of Hurricane Emily toward Bermuda from the southeast. By August 29, when Bermuda was under the cirrus shield of the hurricane, the upper part of the sounding shows very little O₃. The cirrus shield represents the presence of marine boundary layer air in the upper troposphere pumped up and outward from the center of the storm. There is a residual dry layer, with a relative enhancement with respect to the rest of the troposphere, at midtroposphere heights.

4. Discussion

The isentropic trajectory endpoints discussed in the last section were modeled based on the NMC wind fields although the IPV fields were based on an objective analysis of rawinsonde observations. Given the modest resolution of the NMC wind fields, this degree of correspondence or agreement between the ozonesondes with high ozone and transport from regions proximate to high IPV, although not quantitative, is strongly indicative of a stratospheric source for these ozone mixing ratios over Bermuda. Figure 9a and b illustrates the differences in transport associated with changes in ozonesonde chemistry. At 1200 UTC on August 27, the isentropic trajectories indicated very rapid flow from the Pacific Northwest to Bermuda (2.5 days), with subsidence from 300 to 400 hPa as the air parcel decelerated into the anticyclonic circulation over Bermuda. One day later transport at the same θ level shows a similar flow pattern which was actually different in two significant ways. The wind speeds were slower with rising motion and the trajectory did not cross through any regions of high IPV at any point upwind.

These results confirm our hypothesis that the upper level flow patterns necessary for the development of the warm sector transport that advected pulses of anthropogenic air over the NARE study region also provided a mechanism for delivering significant amounts of natural O₃ to the upper troposphere which was ultimately advected to the middle to upper troposphere over the NAO. Further evidence of these dual mechanisms occurring is illustrated in Figure 10 which shows aircraft data for 1400-1800 UTC, August 25. This composite profile illustrates that there were, in fact, two distinct layers of O₃ present. The lower layer was present between 500 and 1000 m above the surface on the morning of August 25 under stable stratification. In this layer O₃ and NO$_y$ were correlated with warm moist air; a peak O₃ concentration of 90 ppbv occurred together with 14 gm kg⁻¹ of water vapor. In addition to this pollution signal, there was a second peak in the O₃ profile, where mixing ratios ranging from 70 to 90 ppbv were anticorrelated with NO$_y$ and water
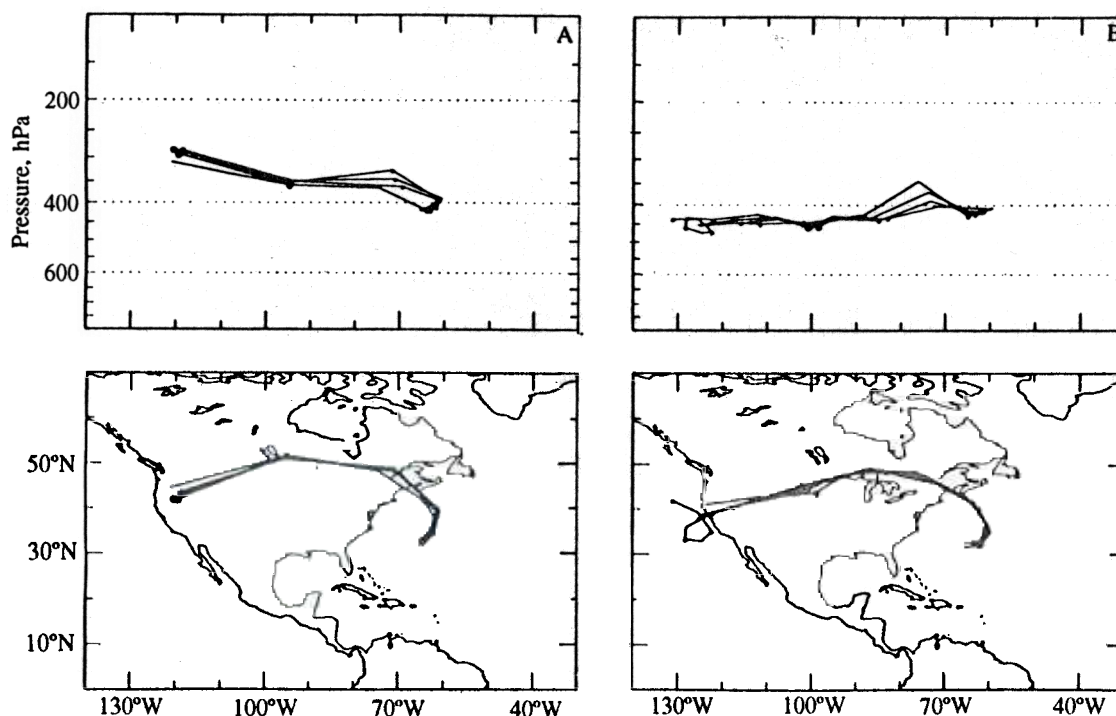
Figure 9. Isentropic back trajectories based on NMC Global Analysis illustrate (a) favorable transport from a region of high IPV and correspond to 86 ppbv observed over Bermuda at 12 UTC, August 27 and (b) transport that does not cross regions of high IPV and corresponds to 50 ppbv observed over Bermuda at 12 UTC, August 28.
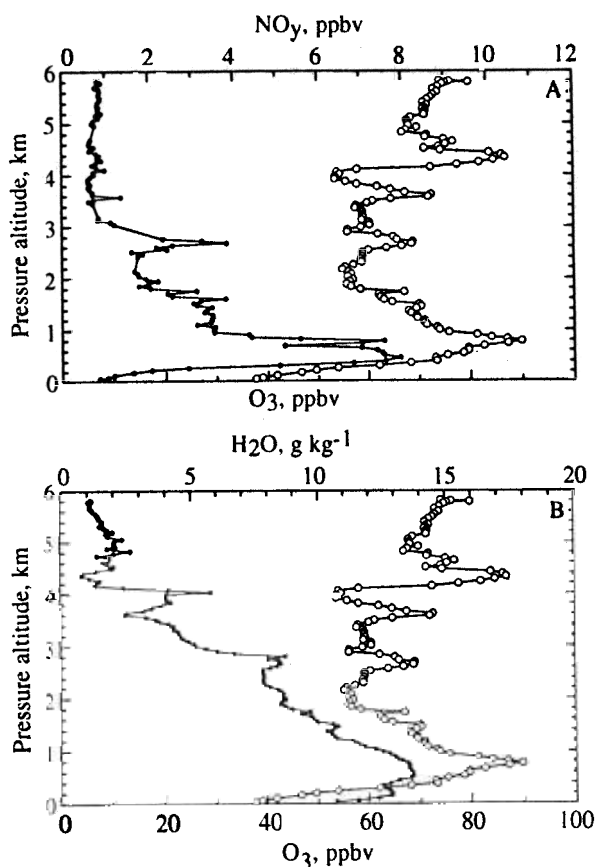
Figure 10. Composite profile from NARE aircraft flight 13 from 1400 to 1800 UTC on August 25, illustrating high concentrations of O_3 (open circles), NO_y (a, closed circles), and water vapor (b, closed circles) in a pollution layer between 500 and 1000 m above the surface. A secondary layer between 4 and 6 km shows high concentrations of O_3 and very dry air, suggestive of a natural source for O_3.

vapor that was of the order of 1 to 2 gm kg^{-1} between 4 and 6 km. Plate 1b suggests that the upper level trough would have moved over the NARE region at this time, with very dry air present in the remotely sensed water vapor signal. In addition, regional scale back trajectories from 4 km over the Gulf of Maine on the afternoon of August 25 indicate transport from the 500-mbar level in the vicinity of upper Michigan and Lake Winnepeg one day earlier. This is the region where the upper air system intensified (as seen in the vorticity maximum and traveling shortwave at 250 mb; Figure 4d). All these results suggest a significant contribution of natural O_3 to midtropospheric levels over the North Atlantic, even in association with the relatively weak baroclinic events typical of summer.

From these analyses we can see that in association with the same systems that advected polluted lower tropospheric air eastward from the continent, there was the potential for a significant amount of natural O_3 transfer to the upper troposphere through exchange mechanisms occurring with tropopause folds. It appears from our analyses of the water vapor images that rapid transport from a tropopause fold over the Pacific Northwest contributed to the high O_3 observed over Bermuda on August 27. The upper air disturbance that generated IPV values greater than 15 (and

transferred stratospheric O_3 into the upper troposphere) went on to spawn the surface frontal system which pushed anthropogenic pollutants over the NARE study region on the August 28. We have not analyzed profiles for other locations over the North Atlantic using IPV as a dynamic tracer. However, it is reasonable to assume that any O_3 associated with high IPV in the troposphere over the continent, or even over the WNAO, could then be advected through the upper troposphere over the midlatitudes of the North Atlantic. As was shown in the interpretation of Bermuda profiles, this O_3 could be transported great distances. Natural ozone exchanged into the upper troposphere then has the potential to reach lower altitudes as air parcels undergo subsidence in regions of anticyclonic motion.

The contribution of stratospheric ozone to the troposphere has long been recognized as significant and there are a number of methods which have been used to estimate the annual average contribution of stratospheric ozone to the northern hemisphere troposphere [e.g., Mohnen et al., 1993]. However, the dynamic nature of these events and their relationship to cyclogenesis serves to emphasize the fact that their distribution is not uniform and we may expect to see significant interannual variations in the contributions from this "source" at various locations.

5. Conclusion

Our analyses show that both natural and anthropogenic sources can deliver high O_3 concentrations (~ 100 ppbv) to the WNAO troposphere, even in the summer. We suggest that the relative importance of these sources in determining the oxidizing capacity of the troposphere and the ozone budget of the WNAO needs further exploration. The data presented here indicate that the ozone budget over the NAO may be significantly influenced by atmospheric dynamics which act to push polluted air of anthropogenic origin out in pulses which are linked to pulses of natural ozone into the upper troposphere upwind of the Atlantic over the continental United States. Even after several days of transport and dilution, these upper tropospheric pulses were observed as significant enhancements of O_3 over Bermuda [see also Merrill et al., this issue].

Since climatological conditions in the summer of 1993 were anomalous in some significant respects, with an upper air pattern which produced a series of waves along a stationary front over the upper Midwest (triggering unprecedented flooding in the Mississippi and Missouri River basins [Kunkel et al., 1994]), it will be important to analyze more events with surface intensives supported by either aircraft or ozonesondes to better diagnose the prevalence and relative significance of the mechanisms described in this paper and to better assess the role of natural ozone in the summertime free troposphere. However, on the basis of meteorological data only, reviewing a routine daily analysis of water vapor and IPV during the summer of 1995 suggests to the author that there was nothing unique about these events and, in fact, suggests this process to be very common throughout the summer. Although we have insufficient chemical data at the present time to demonstrate this relationship, there is good meteorological evidence that water vapor dry bands, like the ribbon of blue which is evident in Plate 1a, may effectively represent rivers of ozone in the upper troposphere.

References

Anderson, B. E., G. L. Gregory, J. D. W. Barrick, J. E. Collins, G. W. Sachse, D. Bagwell, M. C. Shipham, J. D. Bradshaw, and S. T. Sandholm, The impact of U.S. continental outflow on ozone and aerosol distributions over the western Atlantic, *J. Geophys. Res.*, 98, 23,491-23,500, 1993.

Angevine, W., M. Trainer, S. A. McKeen, and C. M. Berkowitz, Mesoscale meteorology of the New England coast, Gulf of Maine, and Nova Scotia: Overview, *J. Geophys. Res.*, this issue.

Appenzeller, C., and H. C. Davies, Structure of stratospheric intrusions into the troposphere, *Nature*, 358, 570-572, 1992.

Danielsen, E. F., and R. S. Hipskind, Stratospheric-tropospheric exchange at polar latitudes in summer, *J. Geophys. Res.*, 85, 393-400, 1980.

Danielsen, E. F., R. S. Hipskind, S. E. Gaines, G. W. Sachse, G. L. Gregory, and G. F. Hill, Three-dimensional analysis of potential vorticity associated with tropopause folds and observed variations of ozone and carbon monoxide, *J. Geophys. Res.*, 92, 2103-2111, 1987.

Draxler, R. R., Hybrid single-particle Lagrangian integrated trajectories (HY-SPLIT): Version 3.0--users guide and model description, *NOAA Tech. Memo, ERL ARL-195*, Natl. Oceanic and Atmos. Admin., Washington, D. C., 1992.

Fehsenfeld, F. C., A. Volz-Thomas, S. Penkett, M. Trainer, and D. D. Parrish, NARE 1993 summer intensive: Foreword, *J. Geophys. Res.*, this issue(a).

Fehsenfeld, F. C., P. Daum, W. R. Leaitch, M. Trainer, D. D. Parrish, and G. Hübler, Transport and processing of O₃ and O₃ precursors over the North Atlantic: An overview of the 1993 summer intensive, *J. Geophys. Res.*, this issue(b).

Hibbard, W., and D. Wiley, An efficient method of interpolating observations to uniformly spaced grids. Preprints in *Conference on Interactive Information and Processing Systems for Meteorology, Oceanography, and Hydrology*, pp. 144-147, Am. Meteorol. Soc., Los Angeles, 1985.

Hoke, J. E., N. A. Philips, G. J. DiMego, J. J. Tucillo, and J. G. Sela, The regional analysis and forecast system of the National Meteorological Center, *Weather Forecasting*, 4, 323-334, 1989.

Holton, J. R., *An Introduction to Dynamic Meteorology*, chap. 7, *Diagnostic analysis of synoptic scale motions in middle latitudes*, Academic, San Diego, Calif., 1972.

Kleinman, L. I., P. H. Daum, Y. N. Lee, S. R. Springston, L. Newman, W. R. Leaitch, C. M. Banic, G. A. Isaac, and J. I. MacPherson, Measurement of O₃ and related compounds over southern Nova Scotia, 1, Vertical distributions. *J. Geophys. Res.*, this issue(a).

Kleinman, L. I., P. H. Daum, S. R. Springston, W. R. Leaitch, C. M. Banic, G. A. Isaac, B. T. Jobson, and H. Niki, Measurement of O₃ and related compounds over southern Nova Scotia, 2, Photochemical age and vertical transport. *J. Geophys. Res.*, this issue(b).

Kley, D. H., H. Geiss, and V. A. Mohnen, Concentrations and trends of tropospheric ozone and precursor emissions in the United States and Europe, *Atmos. Environ.*, 28, 149-158, 1994

Kunkel, K. E., S. A. Changnon, and J. R. Angel, Climatic aspects of the 1993 Upper Mississippi River basin flood, *Bull. Am. Meteorol. Soc.*, 75, 811-822, 1994.

Lamarque, J.-F., and P. G. Hess, Cross-tropopause mass exchange and potential vorticity budget in a simulated tropopause folding, *J. Atmos. Sci.*, 37, 2246-2269, 1994.

Logan, J. A., Tropospheric ozone: Seasonal behavior, trends, and anthropogenic influence, *J. Geophys. Res.*, 90, 10,463-10,482, 1985.

Merrill, J. T., Isentropic airflow probability analysis, *J. Geophys. Res.*, 99, 25,881-25,889, 1994.

Merrill, J. T., and J. L. Moody, Synoptic Meteorology and Transport during the North Atlantic Regional Experiment (NARE) Intensive, *J. Geophys. Res.*, this issue.

Merrill, J. T., R. Bleck, and D. B. Boudra, Techniques of Lagrangian trajectory analysis in isentropic coordinates, *Mon. Weather Rev.*, 114, 571-581, 1986.

Merrill, J. T., J. L. Moody, S. J. Oltmans, and H. Levy II, Meteorological analysis of tropospheric ozone profiles at Bermuda, *J. Geophys. Res.*, this issue.

Mohnen, V. A., W. Goldstein, and W.-C. Wang, Tropospheric ozone and climate change, *Air Waste*, 43, 1332-1344, 1993.

Moody, J. L., S. J. Oltmans, H. Levy, and J. T. Merrill, Transport climatology of tropospheric ozone: Bermuda, 1988-1991, *J. Geophys. Res.*, 100, 7179-7194, 1995.

Oltmans, S. J., and H. Levy, Seasonal cycle of surface ozone over the western North Atlantic, *Nature*, 348, 392-394, 1992.

Oltmans, S. J., and H. Levy, Surface ozone measurements from a global network. *Atmos. Environ.*, 27, 1993.

Oltmans, S. J., et al., Summer and spring ozone profiles over the North Atlantic from ozonesonde measurements, *J. Geophys. Res.*, this issue.

Parrish, D. D., J. S. Holloway, M. Trainer, P. C. Murphy, G. L. Forbes, and F. C. Fehsenfeld, Export of North American ozone pollution to the North Atlantic Ocean, *Science*, 259, 1436-1438, 1993.

Parrish, D. D., J. S. Holloway, and F. C. Fehsenfeld, Routine, continuous measurement of carbon monoxide with parts per billion precision, *Environ. Sci. Technol.*, 28, 1615-1618, 1994.

Shapiro, M. A., Turbulent mixing within tropopause folds as a mechanism for exchange of chemical constituents between the stratosphere and the troposphere, *J. Atmos. Sci.*, 37, 994-1004, 1980.

Shipham, M. C., A. S. Bachmeier, and B. E. Anderson, CITE 3 meteorological highlights, *J. Geophys. Res.*, 98, 23,305-23,324, 1993.

Sirois, A., and J. W. Bottenheim, Use of backward trajectories to interpret the 5-year record of PAN and O₃ ambient air concentrations at Kejimkujik National Park, Nova Scotia, *J. Geophys. Res.*, 100, 2867-2881, 1995.

M. Buhr, J. S. Holloway, D. D. Parish, and M. Trainer, NOAA Aeronomy Laboratory, R/E/Al7, 325 Broadway, Boulder, CO 80303.

J. C. Davenport and J. L. Moody (corresponding author), Department of Environmental Sciences, Clark Hall, Charlottesville, VA 22903. (e-mail: jcd9s@virginia.edu; jlm8h@virginia.edu)

G. L. Forbes, Atmospheric Environment Service, 4905 Dufferin Street, Downsview, Ontario, Canada M3H 5T4.

H. Levy II, NOAA Geophysical Fluid Dynamics Laboratory, Princeton University, Box 308, Princeton, NJ 08542. (email: hl@gfdl.gov)

J. T. Merrill, Center for Atmospheric Chemistry Studies, Graduate School of Oceanography, University of Rhode Island, South Ferry Road, Narragansett, RI 02882-1197.

S. J. Oltmans, NOAA/CMDL/R/E/CG1, 325 Broadway, Boulder, CO 80303. (e-mail: soltmans@cmdl.noaa.gov)